ACS APPLIED MATERIALS & INTERFACES

Research Article

www.acsami.org

Magnetic Binary Metal Oxides Affinity Probe for Highly Selective Enrichment of Phosphopeptides

Mengyi Wang,[†] Chunhui Deng,*[,†] Yan Li,*[,‡] and Xiangmin Zhang[†]

[†]Department of Chemistry and Institutes of Biomedical Sciences, Fudan University, Shanghai 200433, China

[‡]Pharmaceutical Analysis Department, School of Pharmacy, Fudan University, Shanghai 201203, China

Supporting Information

ABSTRACT: In this work, for the first time, binary metal oxides ((Ti−Sn)O_4) were integrated into one entity on an atomic scale on magnetic graphene as affinity probe for highly selective enrichment of phosphopeptides. The newly prepared Fe_3O_4/graphene/(Ti−Sn)O_4 (magG/(Ti−Sn)O_4) composites gathered the advantages of large specific surface area of graphene, superparamagnetism, and biocompatibility of iron oxide, and enhanced affinity properties of binary metal oxides. The phosphopeptide enrichment efficiency of the magG/(Ti−Sn)O_4 composite was investigated, and the results indicated an ultralow detection limit (1 pg/μL or 4.0×10^{-11} M) and an ultrahigh selectivity (weight ratio of β-casein and BSA reached up to 1:1500). Compared with magnetic affinity probes with single metal oxide (magG/TiO_2, magG/SnO_2) or the simple physical mixture of magG/TiO_2 and magG/SnO_2, the magG/(Ti−Sn)O_4 composite possessed stronger specificity, higher selectivity and better efficiency; and more importantly, it possessed the ability to enrich both the mono- and multi- phosophorylated peptides, demonstrating the notable features of the novel binary metal oxides affinity probe in the specific and selective enrichment of phosphopeptides. Additionally, by utilizing the magG/(Ti−Sn)O_4 composites, a total number of 349 phosphorylation sites on 170 phosphopeptides including 66 monophosphopeptides and 104 multiphosphopeptides were captured and identified from mouse brain, indicating the great potential for their application in phosphoproteomics analysis in the future.

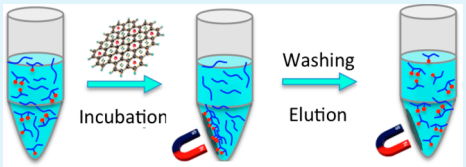

KEYWORDS: *BMOAC, binary metal oxide affinity chromatography, graphene, magnetic, phosphopeptide, enrichment*

INTRODUCTION

Protein phosphorylation is one of the most common and crucial post-translational modifications, which regulates a wide variety of biological processes and cellular activities including signal transduction, cell division, proliferation, differentiation, transformation, and metabolism.[1−7] Owing to the importance of protein phosphorylation, various mass spectrometry (MS)-based methods have been developed to characterize protein phosphorylation.[8−14] However, this task is still of great challenge due to the low abundance and poor ionization efficiency of phosphopeptides, necessitating the enrichment and concentration of phosphopeptides prior to MS analysis. Different affinity-based preseparation techniques and methods have been developed and used for this purpose and metal oxide affinity chromatography (MOAC) is considered more reliable and selective[15−17] among many other pretreatment strategies because of their relatively nonspecific binding to absorbent.

A wide variety of metal oxides (MOs) have been proposed as affinity probes (APs), including TiO_2,[18−23] ZrO_2,[24−28] SnO_2,[29,30] Al_2O_3,[31,32] ZnO,[33] etc., and some of them show complementary preference for monophosphopeptides or multiphosphopeptides. Therefore, APs integrating binary or multi MOs on an atomic scale may exhibit superior enrichment efficiency over APs with single MO (SMOAP).[34,35] However, binary or multi-MO APs have been seldom reported so far.[36−38] Herein, we attempt to develop a facile and universal synthetic route for preparation of AP with binary MOs integrated on an atomic scale, and further investigate the enrichment selectivity and specificity of the binary metal oxide affinity probe (BMOAP).

Graphene has attracted a great deal of interest recently because of its outstanding mechanical and physical properties such as theoretically high specific surface area.[39−41] Graphene decorated with metal materials and metal-oxide nanoparticles has recently been reported.[42−46] Magnetic particles, such as iron-oxide materials,[47] have been extensively used for both in vitro and in vivo application as affinity probes and substrates due to their biocompatibility and superparamagnetism properties resulting in a rapid separation of material-target composites from sample solution.[48,49] Considering the advantages brought by iron-oxide materials and graphene, Fe_3O_4/graphene/TiO_2 composites were prepared in our group for selective enrichment of phosphopeptides in a rapid and convenient way.[50]

In this work, magnetic AP with atomic-scale-integrated binary metal oxides (magG/(Ti−Sn)O_4) were synthesized through a facile and universal synthetic route and applied for phosphoproteomics analysis. The novel magnetic binary metal oxides affinity probe (MBMOAP) gathered the advantages of large specific surface area of graphene, superparamagnetism, and biocompatibility of iron oxide, and enhanced affinity

Received: April 26, 2014
Accepted: June 9, 2014
Published: June 9, 2014

   dx.doi.org/10.1021/am502530c | ACS Appl. Mater. Interfaces 2014, 6, 11775−11782

properties of integrated binary MO. To the best of our knowledge, this is the first MBMOAP integrating Ti and Sn into one entity on an atomic scale on magnetic graphene for enrichment of phosphopeptides. The performances of the obtained MBMOAP were compared with magnetic single metal oxide affinity probe (MSMOAPs) (Fe_3O_4/graphene/TiO_2 and Fe_3O_4/graphene/SnO_2) and the simple physical mixture of Fe_3O_4/graphene/TiO_2 (magG/TiO_2) and Fe_3O_4/graphene/SnO_2 (magG/SnO_2).

RESULTS AND DISCUSSION

Synthesis of Fe_3O_4/Graphene/(Ti−Sn)O_4. The synthesis approach for magG/(Ti−Sn)O_4 composites is shown in Scheme 1. At first, the magnetic graphene was prepared

Scheme 1. Synthetic Approach of Fe_3O_4/Graphene/(Ti−Sn)O_4 Composites

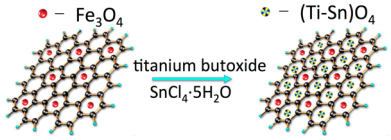

according to a previous method.[51−53] Binary metal oxides ((Ti−Sn)O_4) were then fabricated on the surface of magnetic graphene via simultaneous hydrolysis of titanium butoxide (TBOT) and $SnCl_4·5H_2O$ followed with a calcination treatment procedure. MagG/TiO_2 and magG/SnO_2 were synthesized in a similar way but with hydrolysis of TBOT or $SnCl_4·5H_2O$ only.

Characterization. The morphology of prepared magG/(Ti−Sn)O_4 composites was obtained by transmission electron microscope (TEM), high-resolution transmission electron microscope (HRTEM), and scanning electron microscope (SEM). As demonstrated in Figure 1a, the vertical boundary of

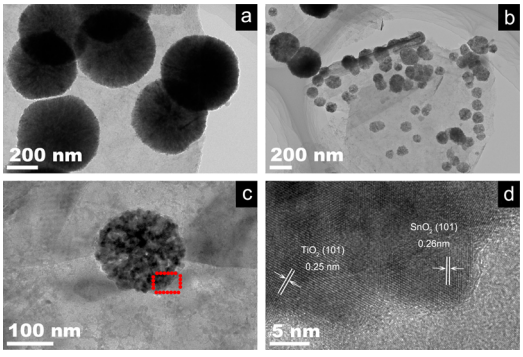

Figure 1. TEM images of (a) magG, (b) magG/(Ti−Sn)O_4, (c) (Ti−Sn)O_4 microspheres on magG/(Ti−Sn)O_4, and (d) HRTEM image of (Ti−Sn)O_4.

graphene is observed and the graphene sheet has a nearly transparent flake-like shape with characteristic crumpled silk waves[54] and single-layer nature. Microspheres with different diameter were observed after calcination treatment to magG/(Ti−Sn)O_4 (Figure 1b). The larger Fe_3O_4 microspheres (~400 nm) have nearly uniform size and spherical shape and exhibit a uniform brightness of image. In contrast, the smaller (Ti−Sn)O_4 microspheres (~250 nm) are observed with uneven brightness of image. The clear differences between these two kinds of microspheres in both diameter and brightness indicate the successful modification of Fe_3O_4 and (Ti−Sn)O_4 on the surface of HNO_3-treated graphene. The HRTEM image exhibit both lattice fringes of 0.25 and 0.26 nm in one single microsphere with smaller diameter and uneven brightness of image (Figure 1d), corresponding to the (101) planes of rutile TiO_2 and (101) planes of tetragonal SnO_2 respectively, indicating that TiO_2 and SnO_2 were not synthesized into two different type of microspheres separately, but formed an integrated binary-MOAP ((Ti−Sn)O_4). Supporting Information Figure S2a displays the energy dispersive X-ray (EDX) spectra of magG/(Ti−Sn)O_4, showing the existence of C, O, Fe, Ti, and Sn elements, further demonstrating the successful synthesis of Fe_3O_4 and (Ti−Sn)O_4 on the graphene sheets. It is worth mentioning that, as shown in Supporting Information Table S1, the molar ratio of Ti and Sn atoms is determined to be 0.12:0.11 by EDX spectra, also confirming the structure of (Ti−Sn)O_4. Similar characterization results of magG/TiO_2 and magG/SnO_2 are given in Supporting Information Figure S2. The BET specific surface area of magG/(Ti−Sn)O_4 was calculated to be 361.5 $m^2·g^{-1}$, while that of magG/TiO_2 and magG/SnO_2 was 191.9 $m^2·g^{-1}$ and 82.6 $m^2·g^{-1}$, respectively, indicating that the magG/(Ti−Sn)O_4 has a relatively high specific surface area. All the results above prove that magG/(Ti−Sn)O_4 composites were successfully synthesized with a relatively high specific surface area, superparamagnetism, and formation of binary metal oxides on an atomic scale, suggesting it promising for highly selective enrichment of phosphopeptides.

Selective Enrichment of Phosphopeptides Using magG/(Ti−Sn)O_4, magG/TiO_2 and magG/SnO_2 Composites. *Selective Enrichment of Phosphopeptide from Tryptic Digests of β-Casein.* To assess the selectivity of magG/(Ti−Sn)O_4, the composites were used to isolate phosphopeptides from tryptic digests of β-casein, a standard phosphorylated protein. A typical procedure to enrich phosphopeptide from a tryptic digest of protein is displayed in Supporting Information Scheme S1. For comparison, two kinds of MSMOAPs (magG/TiO_2 and magG/SnO_2) were also applied to enrich phosphopeptides from tryptic digests of β-casein under the same enrichment condition. When β-casein digest was diluted to 10 ng/μL, no phosphopeptide is detected before enrichment (Figure 2a). As shown in Figure 2b and c, the both MSMOAPs show weak ability for enrichment of multiphosphorylated peptides. Only a weak signal of multiphosphorylated peptide (m/z 3122) can be detected after enrichment with magG/TiO_2, while no multiphosporylated peptide peaks can be observed after enrichment with magG/SnO_2. Although the both MSMOAPs exhibit preference to monophosphorylated peptides (m/z 2061, 2556), differences still exist between them. The signal at m/z 2061 is higher than the signal at m/z 2556 after enrichment with magG/TiO_2, while after enrichment with magG/SnO_2, the signal at m/z 2556 is higher. After enrichment with the simple physical mixture of magG/TiO_2 and magG/SnO_2, the two monophosphopeptides (m/z 2061, 2556) are equally enriched (Figure 2d). However, the signal of multiphosphorylated peptide (m/z 3122) is still weak, indicating that the simple physical mixture of MSMOAPs can not change the enrichment preference and can only slightly improve the enrichment efficiency. In contrast, after enrichment with the newly prepared MBMOAP (magG/(Ti−Sn)O_4), not only the monophosphorylated peptides can be detected with strong intensities but also the signal of multiphosphorylated peptide is greatly improved, indicating the strong enrichment ability of

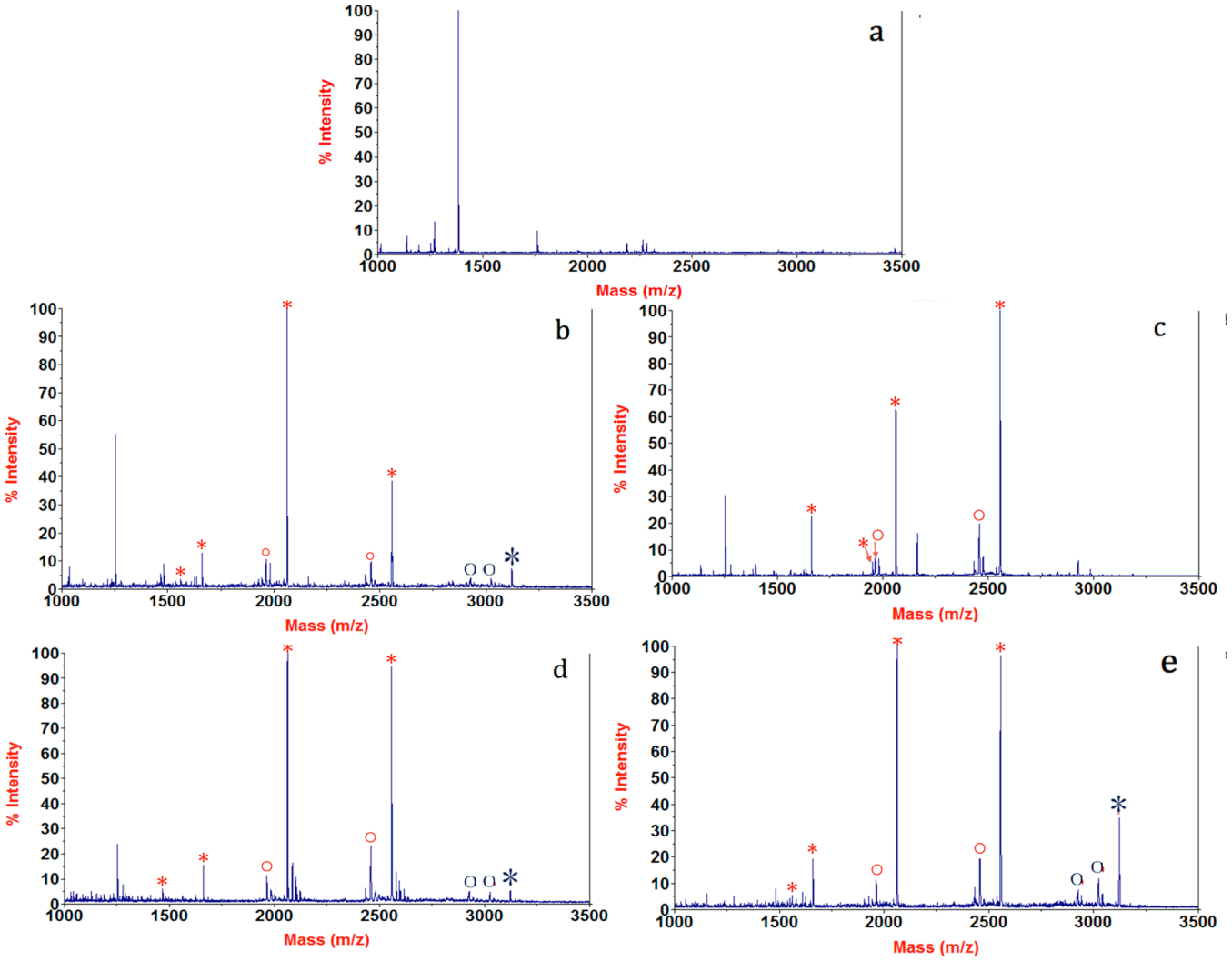

Figure 2. MALDI-TOF mass spectra of tryptic digested β-casein (10 ng/μL): (a) before enrichment and (b–e) after enrichment by (b) magG/TiO_2, (c) magG/SnO_2, (d) physical mixture of magG/TiO_2 and magG/SnO_2, and (e) magG/(Ti–Sn)O_4. Mass spectrometric peaks are marked as monophosphopeptide (*), dephosphorylated fragment (○), multiphosphopeptide (*), and dephosphorylated fragment (○).

the magG/(Ti–Sn)O_4 for both mono- and multiphosphorylated peptides. It is suggested that the enhanced enrichment performance of the magG/(Ti–Sn)O_4 may be attributed to the integration of Ti and Sn on an atomic scale into one entity on Fe_3O_4/graphene.

Limit of Detection. The detection limit of magG/(Ti–Sn)O_4 composites was investigated by loading tryptic digests of β-casein with different concentrations. When β-casein digest was diluted to 10 pg/μL (4.0×10^{-10} M), no phosphopeptide was detected before enrichment (Figure 3a). After enrichment with magG/TiO_2 or magG/SnO_2, only a weak signal of monophosphorylated peptide (m/z 2061) with very low signal-to-noise ratio (S/N) can be observed in the mass spectra (Figure 3b and c). When the simple mixture of magG/TiO_2 and magG/SnO_2 was applied, three peaks assigned to monophosophorylated peptides of β-casein can be detected after enrichment but still with low intensities (Figure 3d). In contrast, when the further diluted β-casein digest (1 pg/μL or 4.0×10^{-11} M, 8.0 fmol) was enriched with the newly prepared magG/(Ti–Sn)O_4, 6 peaks belonging to both mono and multiphosphopeptides and their dephosphorylated fragments can be observed in the spectrum with high intensities (Figure 3e), implying a better capability and enrichment efficiency of the magG/(Ti–Sn)O_4 over not only MSMOAPs such as magG/TiO_2 and magG/SnO_2 composites but also the physical mixture of MSMOAPs. In addition, the detection limit of magG/(Ti–Sn)O_4 composites was also lower than many other latestly reported SMOAP and even BMOAPs materials for enrichment of phosphopeptides,[37,38,50,55] ultimately proving that the obtained magG/(Ti–Sn)O_4 had remarkable properties and performance in phosphopeptide enrichment.

Recyclability of Phosphopeptides Enrichment. Further, the recyclability of magG/(Ti–Sn)O_4 composites was investigated. The used materials were regenerated by washing with 50 μL of 0.4 M ammonia aqueous solution and 50 μL of 50% acetonitrile and 0.1% TFA aqueous solution (v/v) one time each. The regenerated magG/(Ti–Sn)O_4 composites were reused for phosphopeptide enrichment from diluted β-casein digest (5 ng/μL). As shown in Supporting Information Figure S3, after 5 times' recycling, MS spectrum stayed almost identical to that of the first time. The unchanged performance of the magG/(Ti–Sn)O_4 composites toward phosphopeptides indicated the outstanding recyclability of magG/(Ti–Sn)O_4 composites.

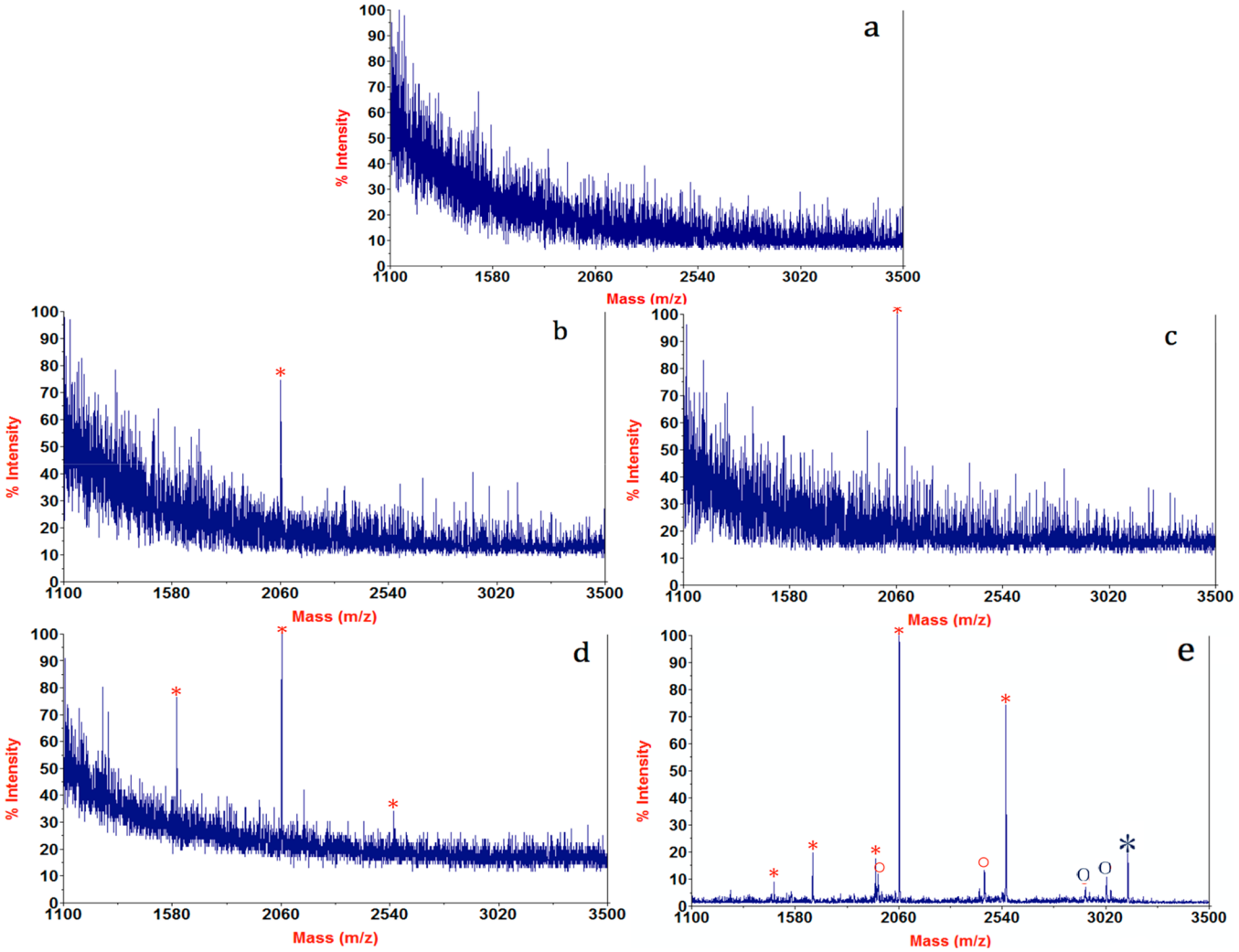

Figure 3. MALDI-TOF mass spectra of tryptic digested β-casein (10 pg/μL (4.0×10^{-10} M)): (a) before enrichment and (b–d) after enrichment by (b) magG/TiO_2, (c) magG/SnO_2, and (d) physical mixture of magG/TiO_2 and magG/SnO_2, and mass spectra of tryptic digested β-casein (1 pg/μL (4.0×10^{-11} M, 8.0 fmol)) (e) after enrichment by magG/(Ti–Sn)O_4. Mass spectrometric peaks are marked as monophosphopeptide (*), dephosphorylated fragment (○), multiphosphopeptide (*), and dephosphorylated fragment (○).

Selective Enrichment of Phosphopeptide from Semicomplex Sample. To further explore the selectivity of magG/(Ti–Sn)O_4 toward phosphopeptides, tryptic digest of BSA, which is a nonphosphorylated protein, was added into that of β-casein in a ratio of 1:10 (w/w) initially. Phosphopeptides could hardly be detected without enrichment (Figure 4a), while after enrichment with magG/(Ti–Sn)O_4, seven peaks of phosphopeptides from β-casein and their dephosphorylated fragments were detected in the mass spectrum with no signals of nonphosphorylated peptides at all (Figure 4b). It is clear that the magG/(Ti–Sn)O_4 composites can specifically and selectively capture phosphopeptides from the semicomplex sample solution, while most of the nonphosphopeptides are removed by washing the composites thoroughly with the help of a magnet. After increasing the weight ratio of β-casein to BSA up to 1:1500, ion signals of phosphopeptides are still prominent in the spectrum and 6 peaks of phosphopeptides as well as their dephosphorylated fragments can be detected despite the signals of nonphosphorylated peptides are also observed (Figure 4c). The results revealed that the magG/(Ti–Sn)O_4 composites had strong specificity, high selectivity, and good efficiency in capturing phosphopeptides from semicomplex sample, suggesting their great potential to enrich phosphopeptides from a complex biological sample.

Selective Enrichment of Phosphopeptide from Complex Biological Sample Mouse Brain. We evaluated the ability of the magG/(Ti–Sn)O_4 composites to selectively extract and enrich phosphopeptides from a real biological sample—mouse brain. After searching the database, the information for the enriched phosphopeptides was obtained. A total number of 349 phosphorylation sites (277 on serine (79.37%), 60 on threonine (17.19%), and 12 on tyrosine (3.44%)) of 170 phosphopeptides including 66 monophosphopeptides and 104 multiphosphopeptides were identified from the mouse brain tissue. The detailed information for the phosphopeptides is listed in Supporting Information Table S2.

The experimental results described above demonstrate that the magG/(Ti–Sn)O_4 composite not only captures a great number of phosphopeptides but also efficiently enriches both the monophosphopeptide and multiphosphopeptide. It has great efficiency in enrichment of phosphopeptides with high sensitivity (the limit of detection as low as 1 pg/μL or 4.0×10^{-11} M) and selectivity toward phosphopeptides in the

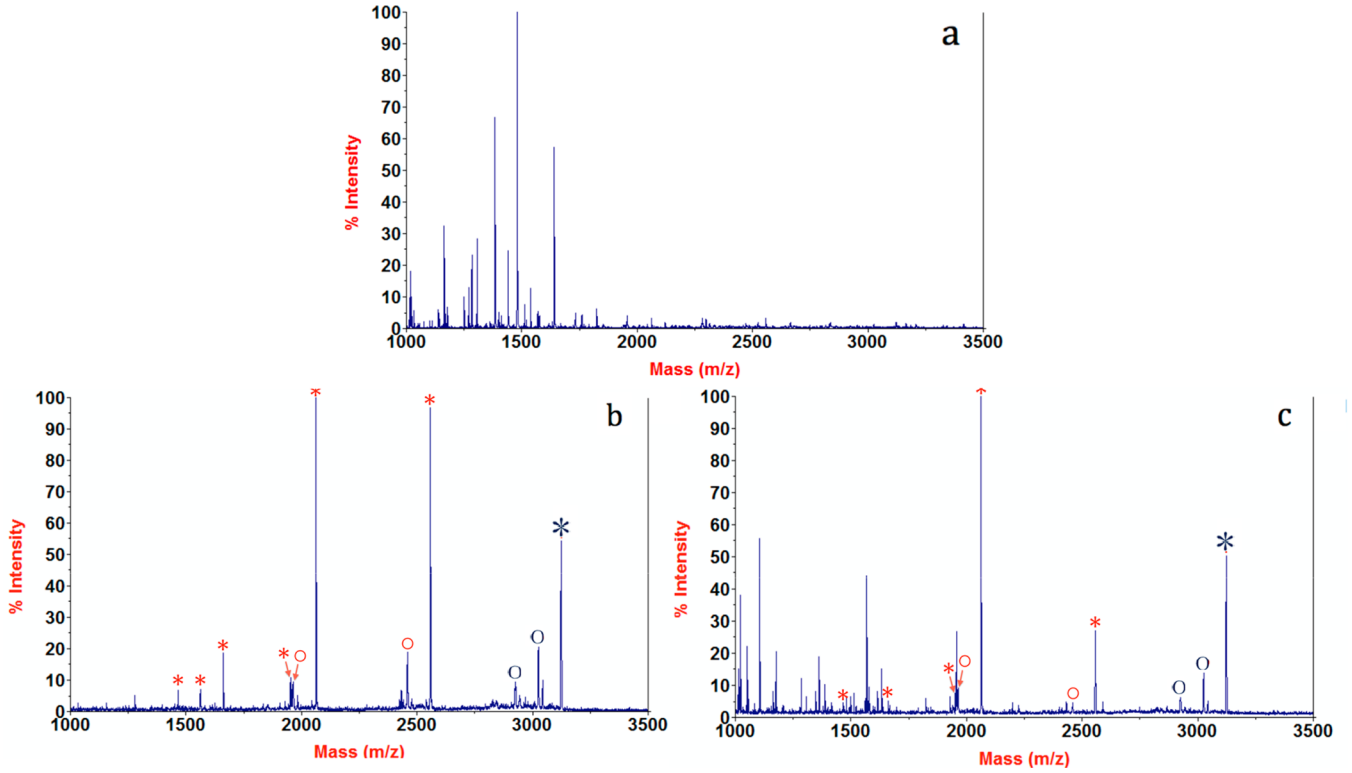

Figure 4. MALDI-TOF mass spectra of peptides derived from peptide mixture of β-casein and BSA (a) before enrichment (in the ratio of 1:10 (w/w)); (b, c) after enrichment in the ratio of (b) 1:10 and (c) 1:1500 (w/w) by magG/(Ti−Sn)O_4. Mass spectrometric peaks are marked as monophosphopeptide (*), dephosphorylated fragment (○), multiphosphopeptide (*), and dephosphorylated fragment (○).

presence of a 1500-fold excess of BSA over β-casein and the complex biological sample mouse brain tissue.

CONCLUSIONS

In summary, a novel magnetic affinity probe magG/(Ti−Sn)O_4 with binary metal oxides were facilely synthesized and applied to selectively enrich phosphopeptides for the first time. To the best of our knowledge, this is the first MBMOAP integrating Ti and Sn into one entity on an atomic scale on magnetic graphene for enrichment of phosphopeptides. The magG/(Ti−Sn)O_4 magnetic composites were utilized to isolate and enrich phosphopeptides from tryptic digest of standard protein β-casein, a semicomplex sample of tryptic digest of β-casein and nonphosphoprotein bovine serum albumin (BSA) and a complex biological sample of mouse brain. The results demonstrated that magG/(Ti−Sn)O_4 possessed stronger specificity, higher selectivity and better efficiency phosphopeptides than magG/TiO_2, magG/SnO_2 or the physical mixture of magG/TiO_2 and magG/SnO_2 and, in particular, showed ability in the enrichment of both the monophosphopeptides and multiphosphopeptides. The limit of detection of magG/(Ti−Sn)O_4 composite was 1 pg/μL (4.0×10^{-11} M, 8.0 fmol), while that of magG/TiO_2, magG/SnO_2 and the physical mixture of magG/TiO_2 and magG/SnO_2 was all 10 pg/μL (4.0×10^{-10} M, 80.0 fmol). The ratio of the semicomplex mixtures of β-casein and BSA reached up to 1:1500 (w/w), and 170 phosphopeptides were captured and identified from the complex biological sample mouse brain tissue. The outstanding performance of magG/(Ti−Sn)O_4 might be attributed to the integration of TiO_2 and SnO_2 into a single binary-metal-oxides microsphere. In conclusion, magG/(Ti−Sn)O_4 composites have notable features in specific and selective enrichment of phosphopeptides and have a great potential to function as an efficient and convenient approach to phosphoproteomics analysis.

METHODS

Materials and Chemicals. Bovine β-casein (from bovine milk), bovine serum albumin (BSA), trypsin (from bovine pancreas, TPCK treated), ammonium bicarbonate (NH_4HCO_3), phenylmethylsulfonyl fluoride (PMSF), and 2, 5-dihydroxybenzoic acid (DHB) were purchased from Sigma Chemical (St. Louis, MO). Iodoacetaamide (IAA) was purchased from Amersham Biosciences (Piscataway, NJ, U.S.A.). DTT, ACN, and TFA were purchased from Merck (Darmstadt, Germany). All aqueous solutions were prepared using Milli-Q water by Milli-Q system (Millipore, Bedford, MA). All other chemicals and reagents were of analytical grade and were purchased from Shanghai Chemical Reagent. Mouse brain tissues were provided by Zhongshan Hospital of Shanghai.

Synthesis of Fe_3O_4/Graphene/(Ti−Sn)O_4. Magnetic graphene was synthesized according to previous methods.[51] Briefly, 400 mg of graphene was dispersed into 50 mL of concerntrated nitric acid with stirring for 6 h, which created carboxylic groups on the outer surface and made it negatively charged. Then, the graphene was collected by centrifugation and washed with Milli-Q water eight times and dried under vacuum at 50 °C. After that, 300 mg of graphene and 200 mg of $FeCl_3 \cdot 6H_2O$ were dispersed into 40 mL of ethylene glycol solution with 0.2 g of trisodium citrate, 2.5 g of sodium acetate, and 1.8 g of poly(ethylene phosphol) under magnetic stirring. The acquired homogeneous solution was sealed in a Teflon-lined stainless-steel autoclave and heated to 200 °C. After 10 h, the autoclave was cooled to room temperature and the obtained magnetic graphene composites collected by magnetic-separation techniques were washed with Milli-Q water and ethanol for three times each.

For the preparation of magG/(Ti−Sn)O_4, 0.50 mL of titanium butoxide (TBOT) and 0.3 g of $SnCl_4 \cdot 5H_2O$ were dissolved in 50 mL of absolute ethanol under ultrasonication for 0.5 h to obtain a homogeneous solution. Subsequently, 0.015 g of the obtained magG

composites was added to the solution with the aid of ultrasonication for 0.5 h. Then, a mixture of water and ethanol (50 mL/10 mL, v/v) was added dropwise into the above suspension under vigorous mechanical stirring within 0.5 h. The mixture was continuously stirred at room temperature for an additional 8 h. After the hydrolysis process was accomplished, the obtained composites were collected with help of a magnet and thoroughly rinsed with water and ethanol. Lastly, the products obtained were dried at 50 °C and calcined in N_2 at 400 °C for 2 h.

Graphene was first treated by HNO_3, which would create carboxylic groups on its outer surface and make it negatively charged. The activated graphene could easily combine with Fe_3O_4 spheres via a simple hydrothermal reaction in the following step. In this hydrothermal reaction, polyethylene phosphol (PEG) was introduced as the capping agent to accelerate the oriented aggregation and to hinder the fast crystal growth by steric configuration. Trisodium citrate was added as a modification in the solution. By these methods, the graphene along with magnetite spheres were capped with citrate groups, resulting in good dispersibility and magnetism of the material in water and ethanol. The magnetic graphene was stable once it had been prepared, and it can be stored for a long time either in suspension or dried form.

Synthesis of Fe_3O_4/Graphene/TiO_2 and Fe_3O_4/Graphene/SnO_2. The procedures for preparation of magG/TiO_2 composites were similar to the synthesis of magG/(Ti−Sn)O_4 except for increasing the amount of titanium butoxide to 1.00 mL and no addition of $SnCl_4{\cdot}5H_2O$.

On the contrary, the amount of $SnCl_4{\cdot}5H_2O$ was increased to 0.60 g and no titanium butoxide was added in the preparation of magG/SnO_2 composites.

Characterization. The morphologies of the prepared magG/(Ti−Sn)O_4, magG/TiO_2 and magG/SnO_2 were investigated by transmission electron microscopy (JEM-2100F) and scanning electron microscopy (XL30) respectively. (The SEM images are shown in Figure S1 in the Supporting Information.) Samples for TEM, SEM, and EDX analysis were prepared by dropping a drop of composites dispersion in ethanol on a Cu grid (Lacey Formvar/Carbon #01883-F, Ted Pella Inc., U.S.A.). The BET specific surface areas were analyzed using adsorption data in a relative pressure range from 0.18 to 0.35.

Preparation of Standard Protein Digests. Bovine β-casein (from bovine milk) and Bovine serum albumin (BSA) were dissolved in 25 mM NH_4HCO_3 buffer (pH = 8.3) and treated with trypsin (2.5%, w/w) for 16 h at 37 °C for direct digestion, respectively. The obtained products were then diluted with 50% acetonitrile and 0.1% TFA aqueous solution (v/v) to certain peptide concentrations.

Preparation of Mouse Brain Lysates. Mouse brain was placed in ice-cold homogenization buffer consisting of 7 M urea, 2 M thiourea, and a mixture of protease inhibitor (1 mM phenylmethanesulphonylfluoride) and phosphatase inhibitors (0.2 mM Na_3VO_4, 1 mM NaF). The mouse brain was homogenized in a Pottter−Elvejhem homogenizer with a Teflon piston after being rinsed to remove blood and minced with scissors, along with 5 mL of the homogenization buffer per 1 g of mouse brain. The suspension was centrifuged at 15 000 rpm for 1.5 h after homogenization for 2 min and vortexed at 0 °C for 0.5 h. The supernatant contained the total mouse brain proteins.

Appropriate volumes of the obtained sample were precipitated, lyophilized to dryness, and redissolved in reducing solution of 6 M guanidine hydrochloride and 100 mM NH_4HCO_3 (pH = 8.3) to adjust the protein concentration to 2 μg/μL. After that, 100 μL of the obtained sample were mixed with 10 μL of 0.5 M DTT and then incubated at 37 °C for 1 h, followed by adding 20 μL of 0.5 M 2-iodoacetamide and incubating for another 0.5 h at 37 °C in the dark. The protein mixtures were exchanged into 50 mM NH_4HCO_3 buffer (pH = 8.5) and digested with trypsin (2.5%, w/w) at 37 °C for 16 h.

Selective Enrichment of Phosphopeptides from Protein Digest and Mouse Brain Lysate. For the standard proteins, the tryptic digests of proteins were first diluted to a certain concentration by binding buffer (50% ACN, 0.1% TFA, (v/v)), and a suspension of composites (400 μg) was added into 200 μL of the peptide solution. The enrichment was performed under gentle agitation at 37 °C for 0.5 h and the pellucid supernatants were removed with the help of magnet. Next, the composites were washed with binding buffer (50% ACN, 0.1% TFA, (v/v)) three times. Finally the enriched peptides were eluted with 5 μL of 0.4 M ammonia aqueous solution for 10 min and analyzed by MALDI-TOF MS.

The tryptic digests of mouse brain were lyophilized and dissolved in loading buffer. Then, 100 μg of composites were added into 400 μL of diluted mouse brain digests and the mixed solutions were shaken at 25 °C for 0.5 h. After that, the materials capturing phosphopeptides were collected with the help of magnet and washed with binding buffer (50% ACN, 0.1% TFA, (v/v)) for three times. Next, the composites were eluted with 50 μL of 0.4 M ammonia aqueous solution for 0.5 h. The eluate was lyophilized, dissolved in 35 μL of loading phase, and submitted for LC-ESI-MS analysis.

Mass Spectrometry and Database Searching. *MALDI-TOF MS Analysis.* For MALDI-TOF MS, 0.6 μL of eluted phosphopeptide solution were deposited on plate using the dried droplet method, followed by another 0.5 μL of DHB matrix solution (20 mg/mL, in 50% acetonitrile and 1% H_3PO_4 aqueous solution (v/v)). MALDI−TOF MS analysis spectra of the peptides were obtained by a 5800 Proteomics Analyzer (Applied Biosystems, U.S.A.) in the positive ion mode with an Nd:YAG laser (383 nm) operated at a repetition rate of 200 Hz and acceleration voltage of 20 kV.

Nano-LC-ESI-MS/MS Analysis. The peptide solution eluted from microspheres were dried thoroughly by lyophilization and then redissolved with aqueous solution (5% ACN, 0.1% formic acid), separated by nano-LC and analyzed by online electrospray tandem mass spectrometry. The experiments were performed on a Nano Aquity UPLC system (Waters Corporation, Milford, U.S.A.), which was connected to an LTQ Orbitrap XL mass spectrometer (Thermo Electron Corp., Bremen, Germany) and equipped with an online nano electrospray ion source (Michrom Bioresources, Auburn, U.S.A.). The separation of the peptides was performed in a SymmetryC18, 5 μm, 180 μm id × 2 cm trap-column and a BEH300 C18, 1.7 μm, 75 μm id × 15 cm reverse phase column (Waters Corporation, Milford, U.S.A.). Other conditions and parameters were selected and set up according to the previous report.[56]

■ ASSOCIATED CONTENT

Supporting Information

Scheme S1, the workflow of phosphopeptides enrichment by using magG/(Ti−Sn)O_4 composites. Figure S1, SEM image of magG/(Ti−Sn)O_4, magG/TiO_2, and magG/SnO_2 composites. Figure S2, the energy dispersive X-ray (EDX) spectrum data of magG/(Ti−Sn)O_4, magG/TiO_2, and magG/SnO_2 composites. Table S1, detail energy dispersive X-ray (EDX) (of Figure S2a) data about element type and percentage of magG/(Ti−Sn)O_4. Table S2, detail information on the phosphopeptides enriched from tryptic digests of mouse brain using magG/(Ti−Sn)O_4. This material is available free of charge via the Internet at http://pubs.acs.org.

■ AUTHOR INFORMATION

Corresponding Authors

*Email: chdeng@fudan.edu.cn.
*Email: yanli@fudan.edu.cn.

Notes

The authors declare no competing financial interest.

■ ACKNOWLEDGMENTS

This work was supported by the 973 Project (2013CB911201, 2012CB910602), the 863 Project (2012AA020202) and the National Natural Science Foundation of China (21075022, 20875017, 21105016).

REFERENCES

(1) Gruhler, A.; Olsen, J. V.; Mohammed, S.; Mortensen, P.; Faergeman, N. J.; Mann, M. O.; Jensen, N. Quantitative Phosphoproteomics Applied to the Yeast Pheromone Signaling Pathway. *Mol. Cell. Proteomics* **2005**, *4*, 310−327.

(2) Pawson, T. Specificity in Signal Transduction: From Phosphotyrosine-SH_2 Domain Interactions to Complex Cellular Systems. *Cell* **2004**, *116*, 191−203.

(3) Lin, T. X.; Chao, C.; Saito, S.; Mazur, S. J.; Murphy, M. E.; Appella, E.; Xu, Y. P53 Induces Differentiation of Mouse Embryonic Stem Cells by Suppressing Nanog Expression. *Nat. Cell Biol.* **2005**, *7*, 165−171.

(4) Thingholm, T. E.; Jensen, O. N.; Larsen, M. R. Analytical Strategies for Phosphoproteomics. *Proteomics* **2009**, *9*, 1451−1468.

(5) Knight, Z. A.; Schilling, B.; Row, R. H.; Kenski, D. M.; Gibson, B. W.; Shokat, K. M. Phosphospecific Proteolysis for Mapping Sites of Protein Phosphorylation. *Nat. Biotechnol.* **2003**, *21*, 1047−1054.

(6) Hubbard, M. J.; Cohen, P. On Target with a New Mechanism for The Regulation of Protein Phosphorylation. *Trends Biochem. Sci.* **1993**, *18*, 172−177.

(7) Hunter, T. Signaling—2000 and Beyond. *Cell* **2000**, *100*, 113−127.

(8) Kalume, D. E.; Molina, H.; Pandey, A. Tackling the Phosphoproteome: Tools and Strategies. *Curr. Opin. Chem. Biol.* **2003**, *7*, 64−69.

(9) Beausoleil, S. A.; Jedrychowski, M.; Schwartz, D.; Elias, J. E.; Villen, J.; Li, J.; Cohn, M. A.; Cantley, L. C.; Gygi, S. P. Large-Scale Characterization of HeLa Cell Nuclear Phosphoproteins. *Proc. Natl. Acad. Sci. U.S.A.* **2004**, *101*, 12130−12135.

(10) Ficarro, S. B.; McCleland, M. L.; Stukenberg, P. T.; Burke, D. J.; Ross, M. M.; Shabanowitz, J.; Hunt, D. F. Phosphoproteome Analysis by Mass Spectrometry and Its Application to *Saccharomyces cerevisiae*. *Nat. Biotechnol.* **2002**, *20*, 301−305.

(11) Chi, A.; Huttenhower, C.; Geer, L. Y.; Coon, J. J.; Syka, J. E. P.; Bai, D. L.; Shabanowitz, J.; Burke, D. J.; Troyanskaya, O. G.; Hunt, D. F. Analysis of Phosphorylation Sites on Proteins from *Saccharomyces cerevisiae* by Electron Transfer Dissociation (ETD) Mass Spectrometry. *Proc. Natl. Acad. Sci. U.S.A.* **2007**, *104*, 2193−2198.

(12) Witze, E. S.; Old, W. M.; Resing, K. A.; Ahn, N. G. Mapping Protein Post-Translational Modifications with Mass Spectrometry. *Methods* **2007**, *4*, 798−806.

(13) Domon, B.; Aebersold, R. Mass Spectrometry and Protein Analysis. *Science* **2006**, *312*, 212−217.

(14) Nita-Lazar, A.; Saito-Benz, H.; White, F. M. Quantitative Phosphoproteomics by Mass Spectrometry: Past, Present, and Future. *Proteomics* **2008**, *8*, 4433−4434.

(15) Resing, K. A.; Ahn, N. G. Protein Phosphorylation Analysis by Electrospray Ionization−Mass Spectrometry. *Methods Enzymol.* **1997**, *283*, 29−44.

(16) Sickmann, A.; Meyer, H. E. Phosphoamino Acid Analysis. *Proteomics* **2001**, *1*, 200−206.

(17) Chi, A.; Huttenhower, C. Analysis of Phosphorylation Sites on Proteins from *Saccharomyces cerevisiae* by Electron Transfer Dissociation (ETD) Mass Spectrometry. *Proc. Natl. Acad. Sci. U.S.A.* **2007**, *104*, 2193−2198.

(18) Pinkse, M. W. H.; Uitto, P. M.; Hilhorst, M. J.; Ooms, B.; Heck, A. J. R. Selective Isolation at The Femtomole Level of Phosphopeptides from Proteolytic Digests Using 2D-Nanolc-ESI-MS/MS and Titanium Oxide Precolumns. *Anal. Chem.* **2004**, *76*, 3935−3943.

(19) Rinalducci, S.; Larsen, M. R.; Mohammed, S.; Zolla, L. Novel Protein Phosphorylation Site Identification in Spinach Stroma Membranes by Titanium Dioxide Microcolumns and Tandem Mass Spectrometry. *J. Proteome Res.* **2006**, *5*, 973−982.

(20) Chen, C. T.; Chen, Y. C. Fe_3O_4/TiO_2 Core/Shell Nanoparticles as Affinity Probes for The Analysis of Phosphopeptides Using TiO_2 Surface-Assisted Laser Desorption/Ionization Mass Spectrometry. *Anal. Chem.* **2005**, *77*, 5912−5919.

(21) Olsen, J. V.; Blagoev, B.; Gnad, F.; Macek, B.; Kumar, C.; Mortensen, P.; Mann, M. Global, In Vivo, and Site-Specific Phosphorylation Dynamics in Signaling Networks. *Cell* **2006**, *127*, 635−648.

(22) Lu, J.; Wang, M. Y.; Li, Y.; Deng, C. H. Facile Synthesis Of TiO_2/Graphene Composites for Selective Enrichment of Phosphopeptides. *Nanoscale* **2012**, *4*, 1577−1580.

(23) Larsen, M. R.; Thingholm, T. E.; Jensen, O. N.; Roepstorff, P.; Jørgensen, T. J. D. Highly Selective Enrichment of Phosphorylated Peptides from Peptide Mixtures Using Titanium Dioxide Microcolumns. *Mol. Cell. Proteomics* **2005**, *4*, 873−886.

(24) Li, Y.; Leng, T.; Lin, H.; Deng, C.; Xu, X.; Yao, N.; Yang, P.; Zhang, X. Preparation of Fe_3O_4@ZrO_2 Core-Shell Microspheres as Affinity Probes for Selective Enrichment and Direct Determination of Phosphopeptides Using Matrix-Assisted Laser Desorption Ionization Mass Spectrometry. *J. Proteome Res.* **2007**, *6*, 4498−4510.

(25) Blacken, G. R.; Volny, M.; Vaisar, T.; Sadilek, M.; Turecek, F. In Situ Enrichment of Phosphopeptides on MALDI Plates Functionalized by Reactive Landing of Zirconium(IV)-*N*-Propoxide Ions. *Anal. Chem.* **2007**, *79*, 5449−5456.

(26) Kweon, H. K.; Hakansson, K. Metal Oxide-Based Enrichment Combined with Gas-Phase Ion-Electron Reactions for Improved Mass Spectrometric Characterization of Protein Phosphorylation. *J. Proteome Res.* **2008**, *7*, 749−755.

(27) Nelson, C. A.; Szczech, J. R.; Xu, Q.; Lawrence, M. J.; Jin, S.; Ge, Y. Mesoporous Zirconium Oxide Nanomaterials Effectively Enrich Phosphopeptides for Mass Spectrometry-Based Phosphoproteomics. *Chem. Commun.* **2009**, 6607−6609.

(28) Du, D.; Liu, J.; Zhang, X.; Cui, X.; Lin, Y. One-Step Electrochemical Deposition of a Graphene-ZrO_2 Nanocomposite: Preparation, Characterization, and Application for Detection of Organophosphorus Agents. *J. Mater. Chem.* **2011**, *22*, 8032−8037.

(29) Sturm, M.; Leitner, A.; Smatt, J.; Linden, M.; Lindner, W. Tin Dioxide Microspheres as a Promising Material for Phosphopeptide Enrichment Prior to Liquid Chromatography-(Tandem) Mass Spectrometry Analysis. *Adv. Funct. Mater.* **2008**, *18*, 2381−2389.

(30) Leitner, A.; Sturm, M.; Hudecz, O.; Mazanek, M.; Smatt, J. H.; Linden, M.; Lindner, W.; Mechtler, K. Probing The Phosphoproteome of Hela Cells Using Nanocast Metal Oxide Microspheres for Phosphopeptide Enrichment. *Anal. Chem.* **2010**, *82*, 2726−2733.

(31) Coletti-Previero, M. A.; Previero, A. Alumina-Phosphate Complexes for Immobilization of Biomolecules. *Anal. Biochem.* **1989**, *180*, 1−10.

(32) Chen, C. T.; Chen, W. Y.; Tsai, P. J.; Chien, K. Y.; Yu, J. S.; Chen, Y. C. Rapid Enrichment of Phosphopeptides and Phosphoproteins from Complex Samples Using Magnetic Particles Coated with Alumina as The Concentrating Probes for MALDI MS Analysis. *J. Proteome Res.* **2007**, *6*, 316−325.

(33) Chen, W. Y.; Chen, Y. C. Functional Fe_3O_4@ZnO Magnetic Nanoparticle-Assisted Enrichment and Enzymatic Digestion of Phosphoproteins from Saliva. *Anal. Bioanal. Chem.* **2010**, *398*, 2049−2057.

(34) Leitner, A. Phosphopeptide Enrichment Using Metal Oxide Affinity Chromatography. *TrAC, Trends Anal. Chem.* **2010**, *29*, 177−185.

(35) Carreon, M. A.; Guliants, V. V. Ordered Meso- and Macroporous Binary and Mixed Metal Oxides. *Eur. J. Inorg. Chem.* **2005**, *2005*, 27−43.

(36) Yan, J.; Li, X.; Cheng, S.; Ke, Y.; Liang, X. Facile Synthesis of Titania-Zirconia Monodisperse Microspheres and Application for Phosphopeptides Enrichment. *Chem. Commun.* **2009**, *20*, 2929−2931.

(37) Li, L. P.; Zheng, T.; Xu, L. N.; Li, Z.; Sun, L. D.; Nie, Z. X.; Bai, Y.; Liu, H. W. SnO_2−$ZnSn(OH)_6$: A Novel Binary Affinity Probe for Global Phosphopeptide Detection. *Chem. Commun.* **2013**, *49*, 1762−176.

(38) Li, W. W.; Deng, Q. L.; Fang, G. Z.; Chen, Y.; Zhan, J.; Wang, S. Facile Synthesis of Fe_3O_4@TiO_2−ZrO_2 and Its Application in Phosphopeptide Enrichment. *J. Mater. Chem. B* **2013**, *1*, 1947−1961.

(39) Stankovich, S.; Dikin, D. A.; Dommett, G. H. B.; Kohlhaas, K. M.; Zimney, E. J.; Stach, E. A.; Piner, R. D.; Nguyen, S. T.; Ruoff, R. S. Graphene-Based Composite Materials. *Nature* **2006**, *442*, 282−286.

(40) Schedin, F.; Geim, A. K.; Morozov, S. V.; Hill, E. W.; Blake, P.; Katsnelson, M. I.; Novoselov, K. S. Detection of Individual Gas Molecules Adsorbed on Graphene. *Nat. Mater.* **2007**, *6*, 652−655.
(41) Pumera, M. Electrochemistry of Graphene: New Horizons for Sensing and Energy Storage. *Chem. Rec.* **2009**, *9*, 211−223.
(42) Liu, J. B.; Fu, S. H.; Yuan, B.; Li, Y. L.; Deng, Z. X. Toward a Universal "Adhesive Nanosheet" for the Assembly of Multiple Nanoparticles Based on a Protein-Induced Reduction/Decoration of Graphene Oxide. *J. Am. Chem. Soc.* **2010**, *132*, 7279−7281.
(43) Kim, Y. K.; Na, H. K.; Lee, Y. W.; Jang, H.; Han, S. W.; Min, D. H. The Direct Growth of Gold Rods on Graphene Thin Films. *Chem. Commun.* **2010**, *46*, 3185−3187.
(44) Liu, F.; Choi, J. Y.; Seo, T. S. DNA Mediated Water-Dispersible Graphene Fabrication and Gold Nanoparticle−Graphene Hybrid. *Chem. Commun.* **2010**, *46*, 2844−2846.
(45) Song, H. J.; Zhang, L. C.; He, C. L.; Qu, Y.; Tian, Y. F.; Lv, Y. J. Graphene Sheets Decorated with SnO_2 Nanoparticles: In Situ Synthesis and Highly Efficient Materials for Cataluminescence Gas Sensors. *Mater. Chem.* **2011**, *21*, 5972−5977.
(46) Li, N.; Liu, G.; Zhen, C.; Li, F.; Zhang, L. L.; Chen, H. M. Battery Performance and Photocatalytic Activity of Mesoporous Anatase TiO_2 Nanospheres/Graphene Composites by Template-Free Self-Assembly. *Adv. Funct. Mater.* **2011**, *21*, 1717−1722.
(47) Nai, R. R.; Blake, P.; Grigorenko, A. N.; Novoselov, K. S.; Booth, T. J.; Stauber, T.; Peres, N. M. R.; Geim, A. K. Fine Structure Constant Defines Visual Transparency of Graphene. *Science* **2008**, *320*, 1308−1308.
(48) Chen, H. M.; Xu, X. Q.; Yao, N.; Deng, C. H.; Yang, P. Y.; Zhang, X. M. Facile Synthesis Of C8-Functionalized Magnetic Silica Microspheres for Enrichment of Low-Concentration Peptides for Direct MALDI-TOF MS Analysis. *Proteomics* **2008**, *8*, 2778−2784.
(49) Lu, J.; Li, Y.; Deng, C. H. Facile Synthesis of Zirconium Phosphonate-Functionalized Magnetic Mesoporous Silica Microspheres Designed for Highly Selective Enrichment of Phosphopeptides. *Nanoscale* **2011**, *3*, 1225−1233.
(50) Lu, J.; Deng, C. H.; Zhang, X. M.; Yang, P. Y. Synthesis of Fe_3O_4/Graphene/TiO_2 Composites for the Highly Selective Enrichment of Phosphopeptides from Biological Samples. *ACS Appl. Mater. Interfaces* **2013**, *5*, 7330−7334.
(51) Jia, B. P.; Gao, L.; Sun, J. *Carbon* **2007**, *45*, 1476−1481.
(52) Deng, H.; Li, X. L.; Peng, Q.; Wang, X.; Chen, J. P.; Li, Y. D. Monodisperse Magnetic Single-Crystal Ferrite Microspheres. *Angew. Chem., Int. Ed.* **2005**, *44*, 2782−2785.
(53) Ge, J.; Hu, Y.; Zhang, T.; Yin, Y. J. Superparamagnetic Composite Colloids with Anisotropic Structures. *J. Am. Chem. Soc.* **2007**, *129*, 8974−8975.
(54) Chang, H. X.; Tang, L. H.; Wang, Y.; Jiang, J. H.; Li, J. H. Graphene Fluorescence Resonance Energy Transfer Aptasensor for the Thrombin Detection. *Anal. Chem.* **2010**, *82*, 2341−2346.
(55) Yan, Y. H.; Zheng, Z. H.; Deng, C. H.; Zhang, X. M.; Yang, P. Y. Facile Synthesis of Ti^{4+}-Immobilized Fe_3O_4@Polydopamine Core−Shell Microspheres for Highly Selective Enrichment of Phosphopeptides. *Chem. Commun.* **2013**, *49*, 5055−5057.
(56) Lu, J.; Wang, M. Y.; Deng, C. H.; Zhang, X. M. Facile Synthesis of Fe_3O_4@mesoporous TiO_2 Microspheres for Selective Enrichment of Phosphopeptides for Phosphoproteomics Analysis. *Talanta* **2013**, *105*, 20−27.